Applied Water Science (2023) 13:208
https://doi.org/10.1007/s13201-023-02012-2

ORIGINAL ARTICLE

Removing lead from water with carboxylate dendrimers and magnetic nanoparticles modified with carboxylate dendrimers

David Rincón-Montón[1] · David Martínez-Salvador[1] · Javier Sánchez-Nieves[1,2,3] · Rafael Gómez[1,2,3] · F. Javier de la Mata[1,2,3] · Jesús Cano[1,2,3]

Received: 3 February 2023 / Accepted: 20 September 2023

Abstract

Contamination of water with heavy metals as lead (Pb^{2+}) is a relevant problematic issue. In this work, we have tested different types of dendritic materials for lead removal from water and further recovery. The systems employed are magnetic nanoparticles (MNP) modified with monocarboxylate and dendritic carboxylate ligands, and they are compared to pristine MNP and carbosilane dendrimers. They are all effective at removing Pb^{2+}, but the key variations are in their recyclability. The usage of a filtering membrane was required for dendrimers, which was significantly degraded by the acidic media. In terms of MNP, those that were covered by dendritic molecules were clearly less damaged in acidic media. Finally, isotherm analysis revealed that Pb^{2+} interacts differently with unmodified and modified MNP.

Keywords Magnetic nanoparticle · Lead removal · Water purification · Carbosilane dendrimer · Magnetic nanoparticle stability

Introduction

Water is the main essential good for humans, and obtaining water of adequate quality for the different uses is a must (Wang et al. 2021). The increase of human population implies an increase in the demand of water for direct human consumption and also for agriculture, stockbreeding and industry. However, this fact involves environmental problems that affect directly the quality of water (Wang et al. 2021).

Heavy metals are an important concern with respect to water pollution. Contamination can arise from natural sources (e.g. arsenic) (Hare et al. 2019) or from human manipulation. Several of them are very toxic in rather low concentrations (e.g. cadmium, mercury, lead) (Masindi and Muedi 2018). In the particular case of lead, it was widely employed in the past decades, as for example in water pipes. Although their uses have been forbidden in most of the countries, still lead pipes can be found in old systems. Hence, avoiding the release of lead to urban water is nowadays a public health problem.

Heavy metals differ in physical and chemical properties, and therefore, purification processes for them are variable, e.g. ion exchange, precipitation, reverse osmosis, electrochemical treatment, filtration, floatation and adsorption (Joseph et al. 2019), (Shen et al. 2019) being the last one the most attractive in the last years. This process consists on coordination of metal ions to functional groups on a material surface (Khan et al. 2020).

Nanotechnology has become very attractive and useful for this particular field due to properties such as high surface area, photosensitivity, electrochemical, optical and magnetic properties and others (Hairom et al. 2021; Jassby et al. 2018; Qu et al. 2013). For water purification, the nanoparticles have to be easily removed from

✉ Javier Sánchez-Nieves
javier.sancheznieves@uah.es

✉ Jesús Cano
jesus.cano@uah.es

[1] Departamento de Química Orgánica y Química Inorgánica, Instituto de Investigación Química "Andrés M. del Río" (IQAR, UAH), Universidad de Alcalá (UAH), Ctra. Madrid-Barcelona Km. 33, 28805 Alcalá de Henares, Madrid, Spain

[2] Networking Research Center on Bioengineering, Biomaterials and Nanomedicine (CIBER-BBN), Instituto de Salud Carlos III, C/ Monforte de Lemos 3-5, 28029 Madrid, Spain

[3] Instituto Ramón y Cajal de Investigación Sanitaria (IRYCIS), Ctra. de Colmenar Viejo, Km. 9, 28034 Madrid, Spain

Published online: 09 October 2023

the medium and magnetic nanoparticles (MNP) are the most suitable for this purpose. Among MNP, iron-based materials, especially, iron oxide NP, are the dominant species (Martinez-Boubeta and Simeonidis 2019; Moosavi et al. 2020; Wadhawan et al. 2020; Zhang et al. 2016) with important affinity to a variety of metals through their Fe–O bridges (Liosis et al. 2021). However, free iron oxide MNP are present as drawbacks that modification of the surface by their interaction with the environment can modify notably their behaviour (aggregation, magnetic properties) (Zia et al. 2016). Thus, modification of the surface with ligands can avoid this problem and if the ligands are able to trap pollutants, the system improves their water purification ability (Khatibikamal et al. 2019).

Multivalent ligands are very attractive for the above application to reinforce the interaction between the substrate and the contaminants. In this way, polymers have also been widely studied for trapping water impurities such as metals (Sajid et al. 2018; Sohail et al. 2020). Within this type of compounds, dendrimers stand out by their globular and well-defined structure, which allow the establishment of better structure/activity relationships than polydisperse polymers (Malkoch and García-Gallego 2020). For water purification, dendrimers have been incorporated to filtration membranes to enhance their efficacy by interaction with their functions (Gao et al. 2013; Li et al. 2017; Liu et al. 2018; Manna et al. 2019) or by creating porous layers onto them (Allabashi et al. 2007; Yuan et al. 2020).

Incorporation of polymers or dendritic ligands to MNP leads to materials that combine properties of both systems (Kim and Park 2017; Yen et al. 2017; Zarei et al. 2018). On the one hand, the adsorption can be improved due to the presence of multivalent ligands on the surface. On the other hand, the magnetic properties are preserved and the system can be separated from a complex mixture by an external magnetic field. These systems may show a synergistic effect between ligand complexation and electrostatic interaction, as proposed for MNP covered with PAMAM dendrimers (Chou and Lien 2011). Also, this type of dendrimer-modified MNP has been applied for extraction of rivaroxaban from biologic human liquids (Parham et al. 2018) or for efficient DNA purification (Tanaka et al. 2012). Our group has recently anchored carbosilane (CBS) dendritic systems (Ortega et al. 2020) to MNP, showing the ability to trap proteins (Prados et al. 2022), viruses (Barrios-Gumiel et al. 2019) or bacteria (Quintana-Sánchez et al. 2021) depending on the type of ligand.

Herein, we have analysed the ability to retain lead cations by CBS dendrimers with carboxylate moieties, MNP covered with multifunctional dendritic carboxylate ligands and with no-functionalized iron oxide MNP. Studies of recovery and stability of dendrimers and MNP have been also carried out. Finally, isotherm analyses were evaluated to determine the type of coordination of lead to the MNP.

Results and discussion

The nanosystems employed to retain lead cations have been the carbosilane (CBS) dendrimer with carboxylate moieties (Galán et al. 2014b) (Fig. S1), the pristine (**MNP-0**) (Barrios-Gumiel et al. 2019), the MNP covered with carboxylate moieties (**MNP-1b**) and the MNP covered with the CBS dendrimer (**MNP-5b**), and their behaviour has been compared. The CBS systems were used as model of a multivalent trapping system, which could be employed as purification system by itself, or alternatively, anchored to a surface, as in the case of **MNP-5b**.

Synthesis of MNP modified with monocarboxylate (MNP-1) and dendritic carboxylate ligands (MNP-1)

Click reactions are very attractive for functionalization of a widespread type of substrates, among other reasons due to the variety of functional groups that are available through this type of reactions (Tremblay-Parrado et al. 2021; Xi et al. 2014). In the particular case of CBS systems, the generation growth is made through the presence of olefin functions, which can also be used for modification of the structure with thiol-ene click reactions (Galán et al. 2014a; Vasquez-Villanueva et al. 2019). In our case the carboxylic groups, as active trapping groups of lead cations, have been introduced by means of thiol-ene addition. On the other hand, since the surface of iron oxide MNP is covered with hydroxyl groups, one of the procedures for their functionalization is by silanization (Bruce and Sen 2005). For these reasons, herein we have designed a ligand and a dendritic ligand containing one $(EtO)_3Si$-moiety in order to anchor it to the MNP and carboxylic groups to retain metal cations (Fig. 1).

Synthesis of carboxylic ligands

The synthesis of the monocarboxylic ligand (**1**) was achieved (Scheme S1) by reaction of 3-mercaptopropionic acid and triethoxyvinylsilane, using DMPA as photoinitiator, under UV irradiation. ^{1}H- and ^{13}C-NMR spectroscopy clearly showed the disappearance of the vinyl groups in triethoxyvinylsilane and the formation of the new chain $SiCH_2CH_2S$ (^{1}H-NMR: 0.91 ppm for $SiCH_2$ and 2.60 ppm for SCH_2; ^{13}C-NMR: 11.8 for $SiCH_2$ and 26.5 ppm for SCH_2) (Fig. S2).

The heterofunctionalized dendrimer (**5**) was produced following a process described in our research group for analogous CBS dendrimers of higher generation (Galán et al. 2014a). In our case (Scheme S2), we started from a dendrimer containing eight allyl groups. Initially only one of these allyl functions was reacted with one mol of cysteamine hydrochloride ($HS(CH_2)_2NH_3Cl$). Next, neutralization and

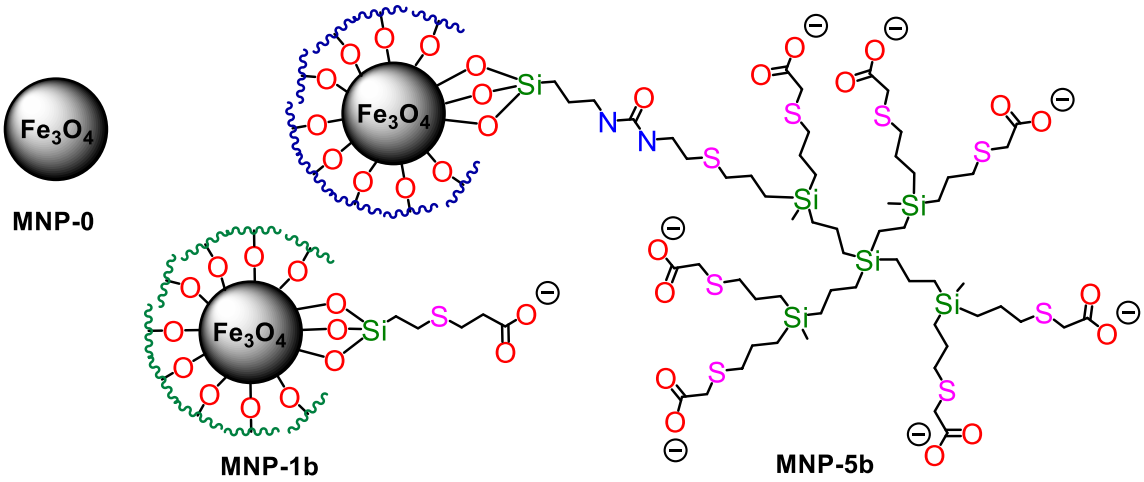

Fig. 1 Drawing of pristine **MNP-0** and MNP modified with monocarboxylate (**MNP-1b**) or dendritic carboxylate ligands (**MNP-5b**)

reaction of the primary amine group with 3-(triethoxysilyl) propyl isocyanate led to a dendrimer with the triethoxysilyl moiety in the outer sphere (**4**). Finally, a second thiol-ene addition of the remaining allyl functions with 3-mercaptopropionic acid afforded the desired dendrimer (**5**).

All these steps were checked by NMR spectroscopy (Figs. S2–S5). The incorporation of the first group was observed by the resonances of the systems $Si(CH_2)_3S$ (similar to ligand **1**) and the new chain introduced SCH_2CH_2N (^{1}H-NMR: 2.91 for SCH_2 and 3.19 for CH_2N; ^{13}C-NMR: 29.4 for SCH_2 and 39.3 ppm for CH_2N). The introduction of the triethoxysilyl moiety was done through formation of a urea bond. The resonances related to this group were the new CH_2N (at *ca.* 3.36 ppm in the ^{1}H NMR spectrum) and the urea carbonyl group (158.9 ppm in the ^{13}C NMR spectrum). The last transformation led to the total disappearance of the allyl resonances and the observation of new alkyl chains $Si(CH_2)_3S$, again similar to ligand (**1**), together with SCH_2CH_2N resonances (2.73 and 2.57 ppm in the ^{1}H NMR spectrum).

Synthesis of carboxylate MNP

The starting Fe_3O_4 MNP were prepared following a well-known procedure described in bibliography (Barrios-Gumiel et al. 2019) (see experimental part). These MNP only contain Fe_3O_4, with no additional ligands on their surface and are named as **MNP-0** for further discussions.

The modification of the **MNP-0** surface with the monofunctionalized carboxylic ligand (**1**) or the dendritic CBS carboxylic ligand (**5**) was done using a 1:1 molar ratio Fe_3O_4:ligand and carried out in EtOH under inert atmosphere. Once these ligands were incorporated to the iron oxide surface, these new MNP (**MNP-1a** and **MNP-5a**) were transformed to carboxylate MNP by addition of excess Na_2CO_3 (Scheme 1 and S3, Fig. 1). The **MNP-1b** and **MNP-5b** thus obtained were characterized by infrared spectroscopy (IR), Z potential, electron microscopy (TEM) and thermogravimetric analysis (TGA) (Figs. S6–S12).

The sizes of the modified MNP were about 12 nm (Figs. 2, S13). With these data and those obtained by TGA (Fig. S12), information about the degree of functionalization of the MNP can be obtained (Table 1). The density of ligands on the MNP surface is higher for the modified MNP with the smaller monofunctional ligand (**MNP-1b**). However, the density of carboxylate moieties is more than twofold for the modified MNP with the dendritic CBS system (**MNP-5b**). Probably, the higher number of carboxylate moieties available in **MNP-5b,** together with the fact that

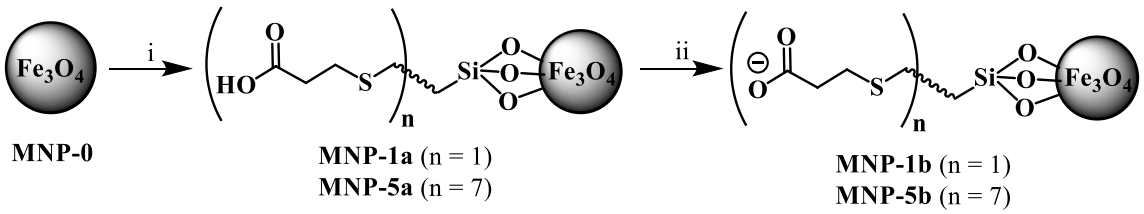

Scheme 1 Synthesis of MNP modified with monocarboxylate ligands (**MNP-1b**) or dendritic CBS carboxylate ligands (**MNP-5b**). (i) **1** or 5 EtOH, 16 h; (ii) Na_2CO_3, H_2O

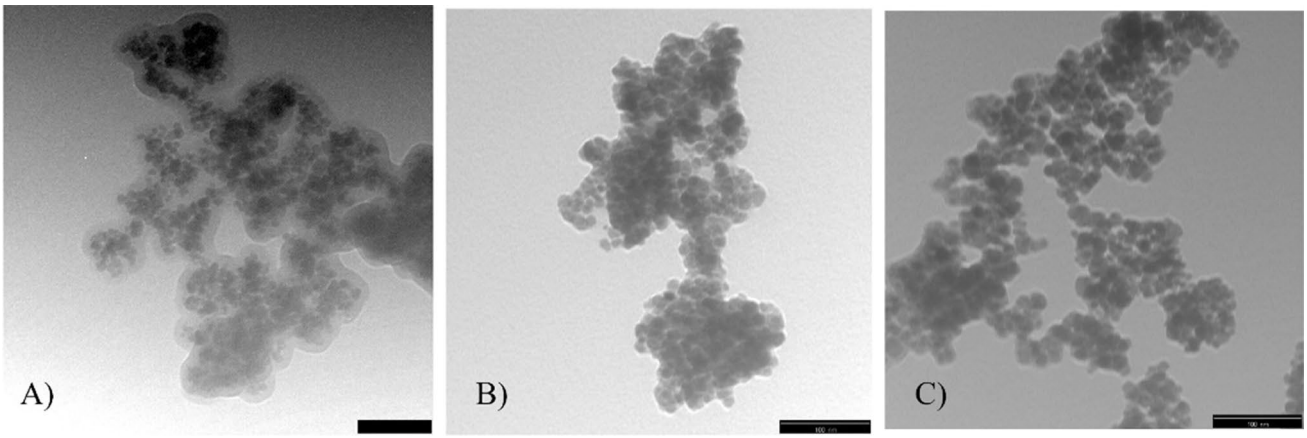

Fig. 2 TEM images of **A MNP-0**, **B MNP-5b** and **C MNP-1b**

Table 1 Data of functionalization of MNP

MNP	Molar ratio[a] Fe_3O_4/L	TGA[b] (% L)	D[c] (nm)	N_L[d]	ρ_L[e] (L/nm^2)	ρ_{func}[f] (CO_2^-/nm^2)	ZP[g] (mV)
MNP-0	–		14.3	–	–	–	−22
MNP-1b	23.8/1	4.9	12.1	524.1	1.14	1.14	−11.6
MNP-5b	70.9/1	9.1	12.2	180.5	0.39	2.70	−20.5

[a]Final molar ratio Fe_3O_4/L obtained by TGA (L = monocarboxylate ligand or dendritic carboxylate ligand)

[b]Mass percentage of ligand in the MNP

[c]Diameter obtained by TEM

[d]Number of functions per MNP

[e]Density of ligands per nm^2

[f]Density of functions per nm^2 (number of functions per ligand: one for monocarboxylate ligand and seven for dendritic ligand)

[g]Z potential

monocarboxylate ligand can fold over the nanoparticle surface decreasing the negative charge in the surface of **MNP-1b**, implicates that the Z potential values were more negative for the dendritic **MNP-5b** than for the **MNP-1b**.

As can be seen in Table 1, the final relationship Fe_3O_4/L is clearly far away from the one used for the synthesis of the modified **MNP-1b** and **MNP-5b**, because the reaction only proceeds on the MNP surface. However, it is necessary to work with such excess to maximize functionalization. With the aim to leverage the excess of dendritic ligand used in the synthesis of the modified **MNP-5b**, the supernatant solution of the reaction was recycled and employed in new synthesis of **MNP-5b**. The amount added of **MNP-0** for the following syntheses was about 10% less than the used in the previous batch in order to keep the same ratio MNP:ligand. The dendritic **MNP-5b** obtained in all these syntheses present same characteristics, the procedure can be repeated several times, and even the solution can be stored for several days before repeating the procedure.

Capture of Pb^{2+} with carboxylate dendrimers

These assays of lead capture with anionic dendrimers G_n-$(CO_2^-)_m$ ($n = 0$, $m = 4$; $n = 1$, $m = 8$; $n = 2$, $m = 16$) (Fig. S1) (Galán et al. 2014b) were done with different relationships $–CO_2^-$:Pb^{2+} (see Table 2). Mixing solutions of terminated carboxylate CBS dendrimers and $Pb(NO_3)_2$ led to formation of white precipitates that were removed from the solution by centrifugation. These solids corresponded with dendrimers complexing Pb^{2+}. The data collected in Table 2 indicated that for all $–CO_2^-$:Pb^{2+} ratios, dendrimers were able to coordinate almost the maximum lead possible but not for G_2-$(CO_2^-)_8$ using a 8:1 relationship. In this case, the high number of carboxylate units not coordinated to lead cations afforded a high concentration of anionic groups making these dendritic systems soluble in water avoiding removal by precipitation.

With the aim to separate dendrimers from extracted Pb^{2+} for their recyclability, a suspension formed with **G_2-$(CO_2^-)_8$**

Table 2 Data of lead capture in with anionic CBS dendrimers G_n-$(CO_2^-)_m$ ($n=0$, $m=4$; $n=1$, $m=8$; $n=2$, $m=16$) obtained by ICP from the remaining lead in solution

	G_0-$(CO_2^-)_4$	G_1-$(CO_2^-)_8$			G_2-$(CO_2^-)_{16}$		
$-CO_2^-:Pb^{2+}$	2:1	4:1	2:1	1:1	8:1	2:1	1:1
Pb^{2+} capture	100.0	98.5	98.9	99.7	63.9	97.1	97.8

and Pb^{2+} ($-CO_2^-:Pb^{2+}$ 8:1) was treated with 0.01 M solution of HNO_3 and filtered through a nanofiltration membrane (1000 kDa). Due to the size of dendrimer, it was retained in the membrane and the filtered solution was analysed by ICP. Less than 2% of lead was recovered from this process, mainly due to the instability of the nanofiltration membrane towards high acidic pH, which is necessary for the decoordination of Pb^{2+} from carboxylic dendrimers. Therefore, the instability of the membrane, the difficulty to separate small dendrimers and the high solubility of formed lead metallodendrimers in low concentrations of lead respect carboxylate groups, moved us to study MNP as support platform to dendrimers for lead removal from water.

Capture of Pb^{2+} with MNP

For this purpose, two types of tests of lead capture were performed, always with a constant Pb^{2+} concentration (16.7 mg/L), using the three MNP, unmodified **MNP-0** and modified **MNP-1b** and **MNP-5b**. In the first assay, the concentrations of each nanoparticle were calculated considering a constant ratio of the Fe_3O_4 core in each MNP respect Pb^{2+}. The chosen concentrations of Fe_3O_4 core in the three MNP were 0.1, 0.2, 0.4 and 0.8 g/L. In the second, the influence of the carboxylate/lead ratio was analysed employing different molar ratios $-CO_2^-:Pb^{2+}$ (1:1, 2:1, 4:1, 8:1). For both types of experiments, the MNP were dispersed in a water solution of $Pb(NO_3)_2$ (pH 6.5) and, after treatment, the supernatant was analysed by ICP to determine the amount of Pb^{2+} retained by MNP.

Regarding experiments of lead capture with respect to Fe_3O_4 concentrations (Fig. 3), the results showed that the capture increased with the amount of Fe_3O_4 present in the solution for all MNP, clearly as a consequence of the higher surface accessible to interact with lead cations. The most active MNP at a sonication time of 1 min was the unmodified **MNP-0**. However, increasing sonication time up to 15 min equals lead capture ability of **MNP-0**

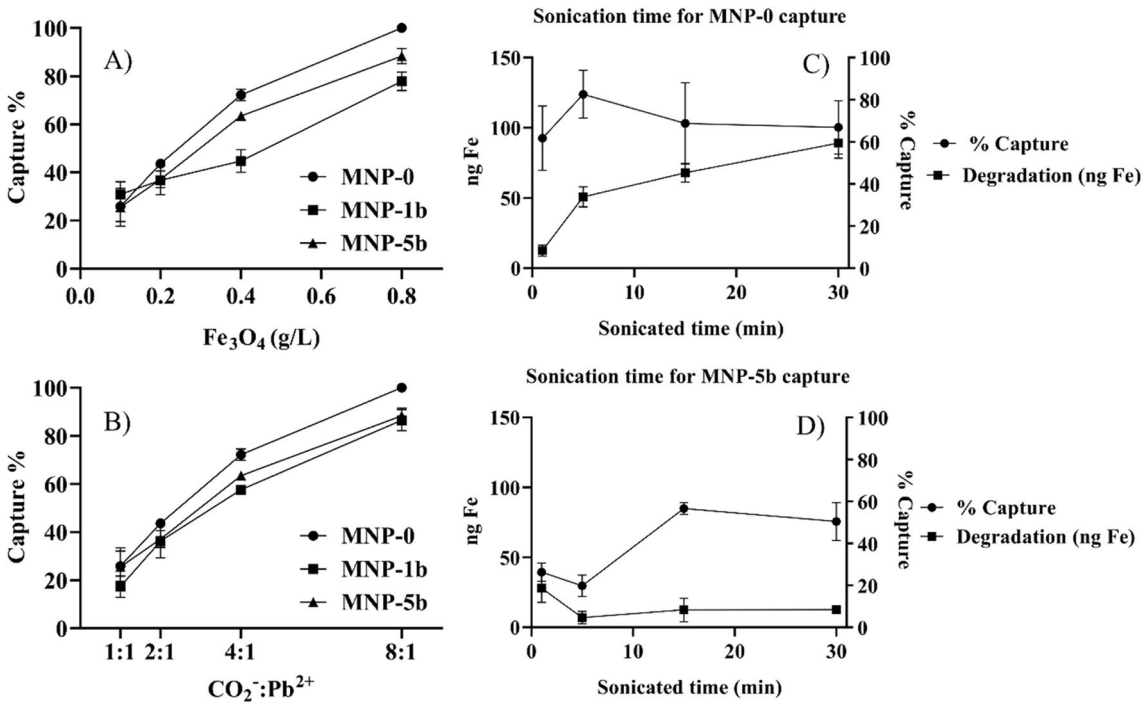

Fig. 3 Pb^{2+} capture with MNP: **A** using equivalent amounts of Fe_3O_4 per MNP; **B** at fixed $-CO_2^-:Pb^{2+}$ relationships (**MNP-0** corresponds with Fe_3O_4 concentrations equal to that present in **MNP-1b**). Optimization of the time that the system is sonicated **C** for **MNP-0** and **D** for **MNP-5b**

and **MNP-5b** while clearly increases degradation of **MNP-0**. On the other hand, it should also be noted that **MNP-1b** recovering from the initial suspension was less efficient, requiring longer magnetic separation time (from 5 to 30 min, Fig. S14).

The results for lead capture with the different $–CO_2^-$:Pb^{2+} ratios (Fig. 3) indicated very similar behaviour for both modified **MNP-1b** and **MNP-5b**. If the carboxylate moiety is considered as the active group, this function behaves similarly independent of being part of a monoligand or of a multiligand. However, as mentioned before, the recovering of **MNP-1b** from suspension was less efficient, needing a longer period to be completed.

MNP recyclability

Since the MNP are easily set aside from the suspension by applying an external magnetic field, it is very interesting to investigate their recyclability. For this purpose, the three MNP, **MNP-0**, **MNP-1b** and **MNP-5b**, containing the lead retained in the previous assays, were treated with HNO_3 (1 M and 3 M) and stirred for 5 and 15 min. Then, the MNP were deposited via an external magnetic field and again the supernatant was analysed by ICP to determine the amount of lead released from the MNP. In Fig. 4A, it can be noticed that the recovery is around 90–100% for all the MNP, the conditions of HNO_3 concentration and agitation time.

These solutions were also tested by ICP to analyse the presence of iron cations to figure out MNP degradation or a possible bad separation (Fig. 4B). As can be expected, degradation increased for higher nitric acid molarity and exposure time. This phenomenon was clearly more noticeable for **MNP-1b**. In this case, it was observed that this MNP dispersed easily than **MNP-0** and **MNP-5b**, so probably interact better with the acidic solution. Moreover, **MNP-1b** precipitated more difficultly from the solution, remaining in the water suspension after magnetic separation. In this experiment, the presence of the dendritic ligand was positive for the longer contact time when a 3 M solution of HNO_3 was employed, since **MNP-5b** were the MNP that were less degraded.

These experiments demonstrate the importance of pH in the interaction of lead cations and the MNP surface. A capture test was done at pH 3.0 and 4.5 with **MNP-0** and **MNP-5b** to confirm this observation. **MNP-1b** were excluded because of its higher degradation, as a consequence of longer magnetic separation times needed for it (as mentioned before). The results showed that at the most acidic pH (3.0), the capture was insignificant because the carboxylic groups and the surface were protonated: 12% for **MNP-0** and 5% for **MNP-5b**. At pH 4.5, capture values of 30% for **MNP-0** and 51% for **MNP-5b** were obtained due to partial protonation of the anionic groups. These data are in accordance

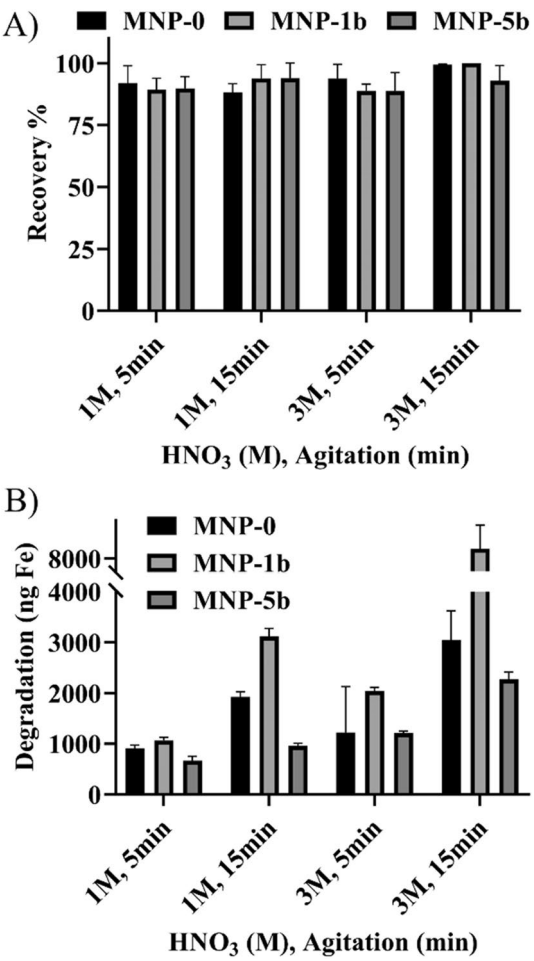

Fig. 4 **A** Percentage of MNP recovered, depending on acid molarity and agitation time. **B** Degradation of MNP after acid treatment (Fe ng determined by ICP)

with the recovery experiments carried out at pH = 0.5, where all the anionic groups are totally protonated and the interaction between MNP and metal cations are broken. Basic pH tests were ruled out since insoluble lead species are formed.

Once the ability of MNP to capture and release $Pb^{2+}$was observed, the possibility to recycle the MNP was tested using **MNP-0** and **MNP-5b**. First, the conditions of sonication time with lead (1 min, Fig. S15), magnetic separation time (20 min, Fig. S16), acid nitric concentration (0.1 M, pH 0.5, Fig. S17) and nitric acid contact time (1 min, Fig. S18) were optimized. Then, the capture and release process was repeated for 10 cycles, starting with 250 µg of MNP in 1.5 mL and 10 µg of Pb^{2+} for each cycle. The release of Pb^{2+} was done with 1.5 mL HNO_3 0.1 M, and the carboxylate groups were recovered with 1.5 mL Na_2CO_3 5 mM. This recycling experiment (Fig. 5) showed that **MNP-5b** was almost no affected during this process, whereas for **MNP-0**, Pb^{2+} capture diminished after 5 cycles. However, in both cases the Pb^{2+} recovery was close to 100%. Regarding

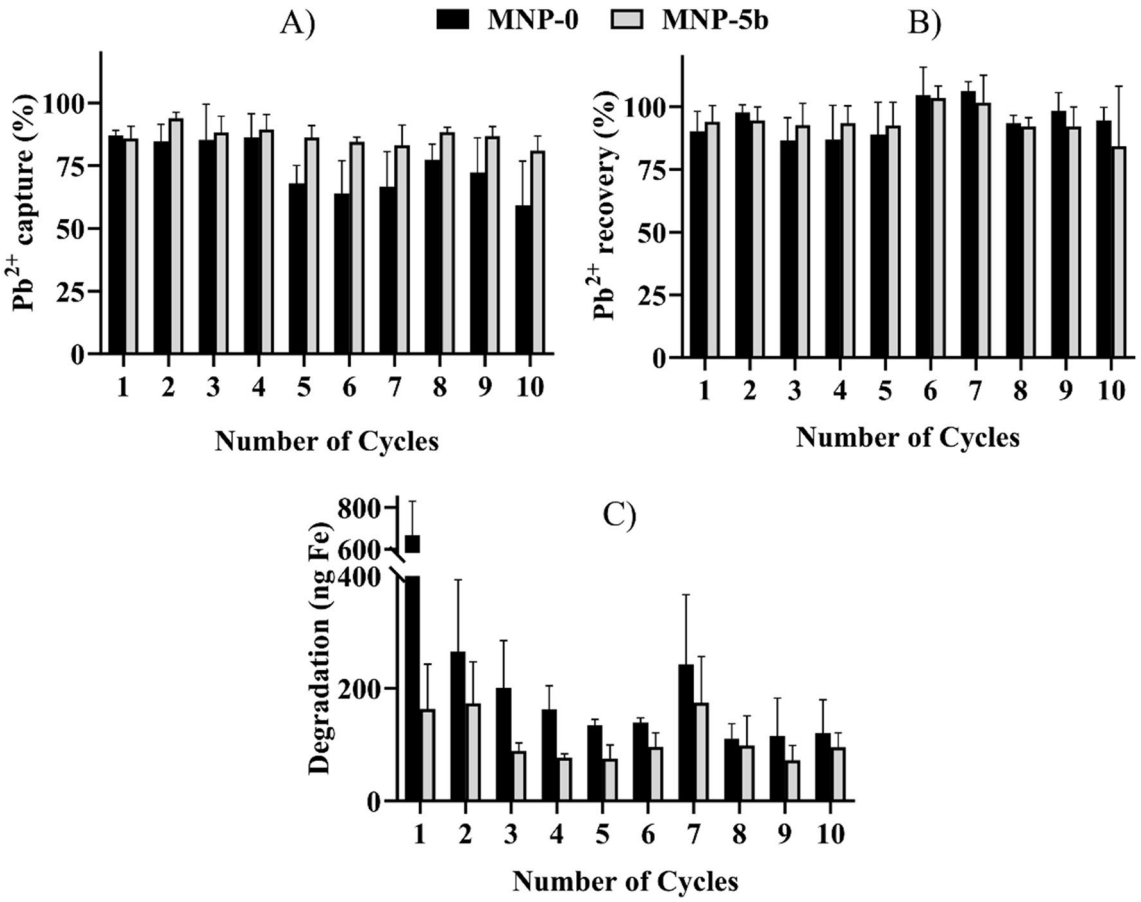

Fig. 5 **A** Percentage of lead captured for each cycle. **B** Percentage of lead recovered. **C** Degradation of the MNP in each step

degradation, Fig. 5C, it was higher during the 10 cycles for **MNP-0** with respect to **MNP-5b**, especially in the first cycle. Apparently, this fact could be fitted with the release of iron cations adsorbed on MNP surface from their synthesis, which must be less strongly attached to the MNP.

Adsorption isotherms

The interaction of the Pb^{2+} cations with the adsorbent MNP can be analysed by their adsorption isotherms. Two of the main models are Langmuir and Freundlich isotherms. Langmuir's model assumes a homogeneous surface, a single cation occupies a single site, there is no lateral interaction between adjacent cations, and if the surface is completely covered, the adsorption reaches the maximum (monolayer adsorption). For the Freundlich model, the surface is heterogeneous and then there are different affinities for the cations depending on the surface site (multilayer adsorption) (Saadi et al. 2015). For these assays we have chosen **MNP-0** and **MNP-5b**.

In the case of adsorption with **MNP-0** (Fig. 6) this process fits better with the Langmuir model, while for **MNP-5b** (Fig. 7) the data support a Freundlich model. While for **MNP-0** lead cations find all interaction sites equal, for **MNP-5b** the presence of the dendrimer on the surface implies different positions, the iron oxide surface and the carboxylate groups.

From these experiments we calculated the maximum absorption of lead for both MNP. In both cases, this value was very similar, 74.7 mg Pb^{2+}/g MNP for **MNP-0** and 74.5 mg Pb^{2+}/g MNP for **MNP-5b**. Apparently, the presence of the dendrimer did not modify the amount of Pb^{2+} on the MNP surface.

Test in saline water

Capture and recovery tests were also carried out in the presence of NaCl and $CaCl_2$ to determine the influence of salt concentration on lead trapping with MNP (**MNP-0** and **MNP-5b**). Figure 8 shows that Pb^{2+} coordinates to the MNP even in very high concentration of both salts (NaCl and $CaCl_2$). However, while increasing concentrations of NaCl hamper Pb^{2+} capture, the presence of $CaCl_2$ did not impact on the capture power of both MNP. Regarding the

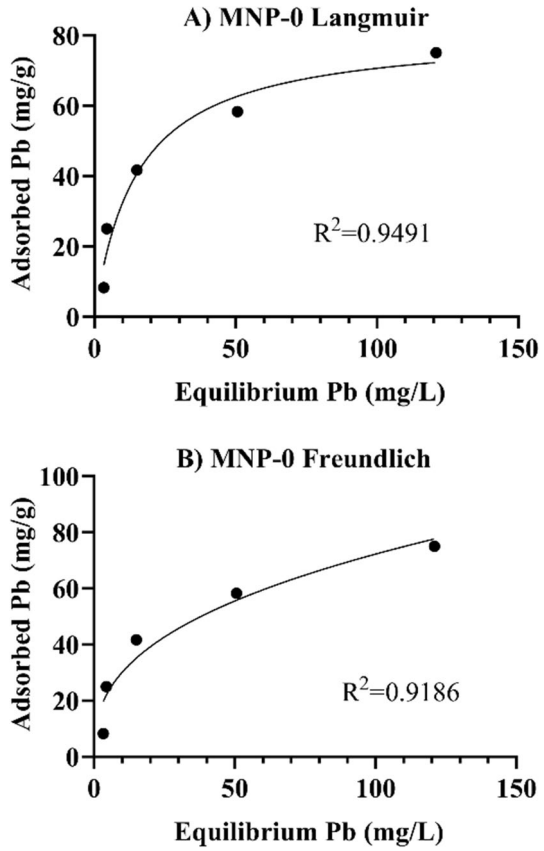

Fig. 6 Adsorption isotherms for **MNP-0**: Langmuir (**A**), Freundlich (**B**)

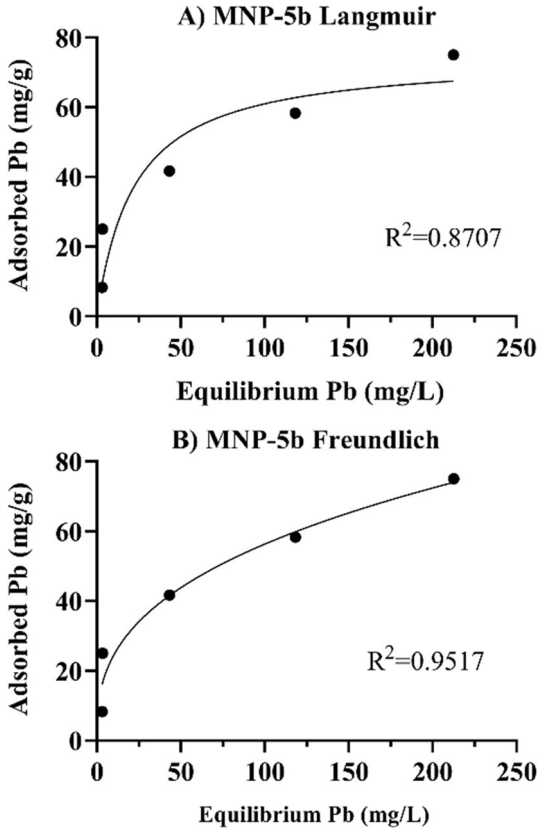

Fig. 7 Adsorption isotherms for **MNP-5b**: Langmuir (**A**), Freundlich (**B**)

preference of Pb^{2+} trapping, it is justified by the softer acid character of Pb^{2+}, which facilitates the establishment of a single covalent bond with the carboxylate anions in **MNP-5b** or with the hydroxyl groups in MNP surface (Pereira et al. 2014). Comparing Na^{+} with Ca^{2+}, both hard acids, possibly the monovalent charge of the sodium cation is more easily compensated by electrostatic interaction with the carboxylate anion or with the hydroxyl groups on the MNP surface, thus affecting more to lead capture (Zheng et al. 2017).

In the recovery process, the saline medium with NaCl does not facilitate the release of Pb^{2+} cations from the MNP surface. However, if $CaCl_2$ is used, the recovery of the MNP improves (Fig. 8).

Conclusions

MNP functionalized with CBS dendrimers containing carboxylate groups in the periphery (**MNP-5b**) have been synthetized, characterized and tested in the removal of lead cations from water. The modified **MNP-5b** have been easily separated from the medium applying a magnetic field, and lead has been removed from the MNP in acidic media. After treatment with a soft base to regenerate the carboxylate groups, these nanosystems have been reused in several cycles maintaining their ability to trap lead, but specially, maintaining their stability. These systems improve the performance of CBS carboxylate dendrimers due to the easiness separation of MNP. Comparing the behaviour of the MNP with a monofunctional ligand (**MNP-1b**) and the MNP modified with a CBS dendrimer (**MNP-5b**), **MNP-1b** degraded easier and precipitated more difficultly from the solution, remaining in the water suspension after magnetic separation hampering their use in the process. Pristine **MNP-0** performed a very good lead-capturing ability, but after some cycles, these MNP started to degrade. The absorption process fits better for **MNP-0** with the Langmuir model, where lead cations find all interaction sites equal, while for **MNP-5b**, the data support a Freundlich model where the presence of the dendrimer on the MNP surface implies different positions, the carboxylate groups and the iron oxide surface. Finally, due to the more covalent nature of the bonds between carboxylate and lead, the MNP clearly retain Pb^{2+} in the presence of large excess of NaCl or $CaCl_2$, even about 1000 fold than $Pb(NO_3)_2$, as found in salt water.

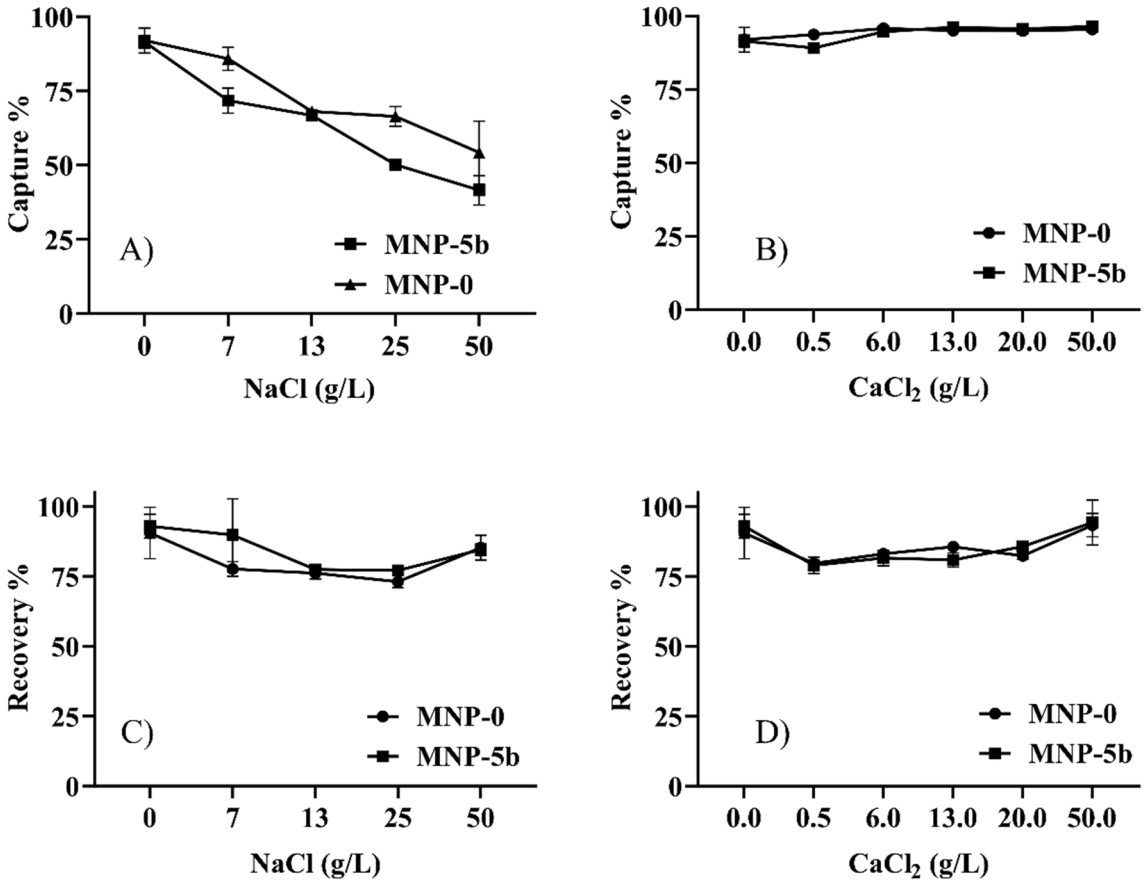

Fig. 8 Influence of NaCl and $CaCl_2$ concentration on Pb^{2+} capture (**A**, **B**) and recovery (**C**, **D**) ($[Pb^{2+}] = 16.7$ mg/L)

Experimental section

Methodology

The synthesis of the ligands or dendrimers and its functionalization were carried out under inert conditions using dry solvents. Triethoxyvinylsilane (Merck, 97%), 3-mercaptopropionic acid (Aldrich, > 99%), DMPA (Acros Organics, 99%), 2-aminoethanethiol hydrochloride (Acros Organics, 98%), Na_2CO_4 (Panreac, pure), (3-isocyanatopropyl)triethoxysilane (Alfa Aesar, 95%), triethylamine (Thermo Scientific, 99.7%), $FeCl_2{\cdot}4H_2O$ (Panreac, pure) and $FeCl_3{\cdot}6H_2O$ (Sigma-Aldrich, > 99%) were obtained from commercial sources. Carboxylate dendrimers were synthesized according to the literature (Barrios-Gumiel et al. 2019; Galán et al. 2014b). The NMR spectra (Nuclear Magnetic Resonances) ^1H and ^{13}C, HSQC (Heteronuclear Single Quantum Correlation), HMBC (Heteronuclear Multiple Bond Correlation) and DOSY (Diffusion-Ordered Spectroscopy) were recorded on Bruker Avance Neo 400 at ambient temperature. The elemental analyses were carried out on a PerkinElmer 240C instrument, UV–Vis measurements using UV–Vis spectrophotometer PerkinElmer Lambda 35 and mass spectra in a Thermo Scientific, TSQ Quantum LC–MS. The amount of metals in the supernatant were analysed by an ICP Varian 720-ES instrument. IR spectra were obtained in a PerkinElmer spectrometer, and to obtain the TEM images, a ZEIS EM TEM equipment with 30-µm lenses and 1-K CCD camera on the lateral was used.

Synthesis of compounds and MNP

Monofunctional ligand $(EtO)_3Si(CH_2)_2S(CH_2)_2CO_2H$ (1)

A dry THF solution of triethoxyvinylsilane (525 mg, 2.76 mmol, 1 equiv), 3-mercaptopropionic acid (242 µL, 2.70 mmol, 1 equiv) and DMPA (2%) was stirred under ultraviolet light for 1 h. Afterwards, the volatiles were removed under vacuum and compound **1** was obtained as yellowish oil, which was used without additional purification for next reaction steps (yield 95%). Data for **1**: ^1H NMR ($(CD_3)_2CO$) δ: 0.95 (t, 2H, SCH_2CH_2Si), 1.20 (t, 2H, OCH_2CH_3), 2.64 (m, 4H, SH_2), 2.77 (t, 2H, $COCH_2CH_2S$), 3.80 (q, 3H, OCH_2CH_3) $^{13}C\{^1H$ NMR ($(CD_3)_2CO$) δ: 11.8 (SCH_2CH_2Si), 18.4 (OCH_2CH_3), 26.5 ($COCH_2CH_2S$), 26.5 (SCH_2CH_2Si), 34.6 ($SOCH_2CH_2Si$), 58.7 (OCH_2CH_3), 177.5

(CO). Elemental analysis for $C_{11}H_{24}O_5SSi$ (296.11 g/mol): Calcd.: C, 44.57; H, 8.16; O, 26.98; S, 10.81; Si, 9.47.

$G_1Si(A)_7(Si(OEt)_3)$ (4)

This compound was obtained following the synthetic routes described below. The intermediate compounds **2** and **3** were not isolated, and NMR characterization was done to confirm the formation of these intermediates. These steps are described as follows:

(a) **$G_1Si(A)_7(S\text{-}NH_3Cl)$** (**2**): Compound **2** was prepared from G_1SiA_8 (403 mg, 0.50 mmol, 1 equiv), 2-aminoethanethiol hydrochloride (58 mg, 0.50 mmol, 1 equiv) and DMPA (2%) in a solution of THF:MeOH (3:1). The solution was stirred and irradiated with ultraviolet light during 30 min. Afterwards, volatiles were removed under vacuum leading to a yellowish oil which was used for the next step. Data for **2**: ^{1}H NMR ($CDCl_3$) δ: − 0.04 (s, 12H, $SiCH_3$), 0.51–0.62 (m, 18H, $SiCH_2CH_2$), 1.31 (m, 8H, $SiCH_2CH_2CH_2Si$), 1.52 (d, 14H, $SiCH_2CHCH_2$), 1.56 (m, 2H, $SiCH_2CH_2CH_2S$), 2.57 (t, 2H, $SiCH_2CH_2CH_2S$), 2.91 (t, 2H, $SCH_2CH_2NH_3$), 3.19 (t, 2H, $SCH_2CH_2NH_3$), 4.80 (dd, 14H, $SiCH_2CHCH_2$), 5.74 (m, 7H, $SiCH_2CHCH_2$), 8.32 (s, 3H, NH_3); $^{13}C\{^1H\}$ NMR ($CDCl_3$) δ: − 5.7 ($SiCH_3$), 13.6 ($SiCH_2CH_2$), 17.8 ($SiCH_2CH_2$), 18.5 ($SiCH_2CH_2$), 18.7 ($SiCH_2CH_2CH_2Si$), 21.8 ($SiCH_2CHCH_2$), 24.4 ($SiCH_2CH_2CH_2S$), 29.4 ($SiCH_2CH_2N$), 35.8 ($SiCH_2CH_2CH_2S$), 39.3 ($SiCH_2CH_2N$), 113.4 ($SiCH_2CHCH_2$), 135.2 ($SiCH_2CHCH_2$). Elemental analysis for $C_{41}H_{82}NSSi_5Cl$ (795.47 g/mol): Calcd: C, 61.78; H, 10.37; N, 1.76; S, 4.02; Obt: C, 61.97; H, 9.36; N, 4.23; S, 3.33.

(b) **$G_1Si(A)_7(S\text{-}NH_2)$** (**3**): A THF/MeOH (1:1) solution of compound **2** (344 mg, 0.43 mmol, 1 equiv) and excess of Na_2CO_4 (5 equivalents per carboxyl group) was stirred during 1 h. The solvent was removed under vacuum to obtain white solid. This solid was dissolved in ether and filtered. Then, the solvent was removed under vacuum obtaining **3** as yellowish oil (96%). Data for **3**: ^{1}H NMR ($CDCl_3$) δ: − 0.04 (s, 12H, $SiCH_3$), 0.51–0.63 (m, 18H, $SiCH_2CH_2$), 1.31 (m, 8H, $SiCH_2CH_2CH_2Si$), 1.53 (d, 14H, $SiCH_2CHCH_2$), 1.58 (m, 2H, $SiCH_2CH_2CH_2S$), 2.49 (m, 2H, $SiCH_2CH_2CH_2S$), 2.58 (m, 2H, $SCH_2CH_2NH_2$), 2.85 (t, 2H, $SCH_2CH_2NH_2$), 4.83 (dd, 14H, $SiCH_2CHCH_2$), 5.75 (m, 7H, $SiCH_2CHCH_2$; $^{13}C\{^1H\}$0.0 NMR ($CDCl_3$) δ: − 5.4 ($SiCH_3$), 13.6 ($SiCH_2CH_2$), 17.8 ($SiCH_2CH_2$), 18.5 ($SiCH_2CH_2$), 18.7 ($SiCH_2CH_2CH_2Si$), 22.0 ($SiCH_2CHCH_2$), 24.8 ($SiCH_2CH_2CH_2S$), 36.0 ($SiCH_2CH_2CH_2S$), 36.7 ($SiCH_2CH_2N$), 41.6 ($SiCH_2CH_2N$), 113.4 ($SiCH_2CHCH_2$), 135.2 ($SiCH_2CHCH_2$). Elemental analysis for $C_{41}H_{81}NSSi_5$ (759.49 g/mol): Calcd: C, 64.75; H, 10.37; N, 1.84; S, 4.22; Obt: C, 64.97; H, 10.32; N, 1.75; S, 2.56.

(c) **$G_1Si(A)_7(Si(OEt)_3)$** (**4**): Under an inert atmosphere, compound **3** (313 mg, 0.41 mmol, 1 equiv) dissolved in THF, (3-isocyanatopropyl)triethoxosilane (105 µL, 0.41 mmol, 1 equiv) and triethylamine (57 µL, 0.41 mmol) were stirred during 16 h. Then the solvents were removed under vacuum obtaining compound **4** as yellowish oil (51%). Data for **4**: ^{1}H NMR ($(CD_3)_2CO$) δ: 0.01 (s, 12H, $SiCH_3$), 0.57 (m, 2H, $NCH_2CH_2CH_2Si$), 0.67 (m, 20H, $SiCH_2CH_2$), 1.19 (t, 9H, OCH_2CH_3), 1.45 (m, 8H, $SiCH_2CH_2CH_2Si$), 1.59 (d, 14H, $SiCH_2CHCH_2$), 1.62 (m, 2H, $SiCH_2CH_2CH_2S$), 1.71 (m, 2H, $NCH_2CH_2CH_2Si$), 2.57 (m, 2H, $SiCH_2CH_2CH_2S$), 2.64 (m, 2H, SCH_2CH_2N), 3.10 (m, 2H, $NCH_2CH_2CH_2Si$), 3.36 (t, 2H, SCH_2CH_2N), 3.81 (q, 6dH, OCH_2CH_3), 4.84 (dd, 14H, $SiCH_2CHCH_2$), 5.81 (m, 7H, $SiCH_2CHCH_2$); $^{13}C\{^1H\}$ NMR ($(CD_3)_2CO$) δ: − 5.5 ($SiCH_3$), 8.2 ($NCH_2CH_2CH_2Si$), 13.8 ($SiCH_2CH_2$), 18.4 (OCH_2CH_3), 18.2 ($SiCH_2CH_2$), 18.8 ($SiCH_2CH_2CH_2Si$), 19.6 ($SiCH_2CH_2$), 23.9 ($SiCH_2CHCH_2$), 24.5 ($SiCH_2CH_2CH_2S$), 26.0 ($NCH_2CH_2CH_2Si$), 31.9 ($SiCH_2CH_2N$), 36.0 ($SiCH_2CH_2CH_2S$), 43.4 (NCH_2), 46.0 (NCH_2), 58.8 (OCH_2CH_3), 113.5 ($SiCH_2CHCH_2$), 135.8 ($SiCH_2CHCH_2$), 158.9 (CO). Elemental analysis for $C_{51}H_{102}N_2O_4SSi_6$ (1006.62 g/mol); Calcd: C, 60.77; H, 10.20; N, 2.78; O, 6.35; S, 3.18; Si, 16.72.

$G_1Si(CO_2H)_7(Si(OEt)_3)$ (5)

To a THF solution of compound **4** (210 mg, 0.21 mmol) under inert conditions were added 3-mercaptopropionic acid (127 µL, 1.47 mmol, 7 equiv) and DMPA (2%). The solution was stirred and irradiated under ultraviolet light during 4 h. Then the solvents were removed under vacuum obtaining a yellowish oil that was used in situ for MNP functionalization. Data for **5**: ^{1}H NMR ($(CD_3)_2CO$) δ: 0.01 (s, 12H, $SiCH_3$), 0.65 (m, 34H, $SiCH_2$), 1.15 (t, 9H, OCH_2CH_3), 1.41 (m, 8H, $SiCH_2CH_2CH_2Si$), 1.60 (m, 16H, $SiCH_2CH_2CH_2S$), 1.76 (m, 2H, $NCH_2CH_2CH_2Si$), 1.91 (t, 4H, H), 2.57 (m, 30H, SCH_2), 2.73 (m, 16H, SCH_2CH_2N, SCH_2CH_2CO), 3.09 (m, 2H, $NCH_2CH_2CH_2Si$), 3.31 (m, 2H, SCH_2CH_2N), 3.76 (m, 6H, OCH_2CH_3). $^{13}C\{^1H\}$ NMR ($(CD_3)_2CO$) δ: − 5.6 ($SiCH_3$), 7.4 (C), 13.2 (C), 17.4 (C), 17.8 (C), 17.9 (C), 18.6 (C), 19.1 (C), 24.3 (C), 26.6 (C), 34.4 (C), 35.4 (C), 37.7 (C), 56.7 (NCH_2), 57.9 (NCH_2), 172.4 (CO). Elemental analysis for $C_{65}H_{130}N_2O_{18}S_8Si_6$ (1650.57 g/mol); Calcd: C, 47.24; H, 7.93; N, 1.70; O, 17.42; S, 15.52; Si, 10.20.

MNP-0

The coprecipitation method was used to prepare these MNP. $FeCl_2{\cdot}4H_2O$ (478 mg, 2.42 mmol, 1 equiv) and $FeCl_3{\cdot}6H_2O$ (1313 mg, 4.86 mmol, 2 equiv) were dissolved in distilled water under inter atmosphere. Then 17.5 ml of ammonia solution (35%) was added drop by droop. The solution was stirred for 2 h at 90 °C. The black precipitated was washed three times with water and other three more with ethanol (yield 95%). Separation of **MNP-0** from suspension can be done with a magnet or by centrifugation. Data for **MNP-0**: TGA (%): (Fe_3O_4) 96.6, (L) 3.4; ζ potential: − 22.0 mV; mean diameter core (TEM): $D = 14.3$ nm.

MNP@$(CO_2H)_1$ (MNP-1a)

For 10 min an ethanol suspension of **MNP-0** (127 mg, 0.54 mmol) was sonicated. Then was added the THF solution of compound 1 (163 mg, 0.54 mmol), and the suspension was sonicated again for 10 min. The mixture was stirred for 16 h at room temperature, and then the solid was washed 3 times with ethanol, 3 more with water and dried under vacuum (**MNP-1a**, 62%) (separation of MNP from suspension can be done with a magnet or by centrifugation). Data for **MNP-1a**: TGA (%): (Fe_3O_4) 93.5, (L) 5.4; ζ potential: − 16.7 mV; mean diameter core (TEM): $D = 13.4$ nm.

MNP@$(CO_2H)_7$ (MNP-5a)

These MNP were prepared as described above, starting from **5** (562 mg, 0.34 mmol) and **MNP-0** (79 mg, 0.34 mmol) (**MNP-5a**, 64%). Data for **MNP-5a**: TGA (%): (Fe_3O_4) 88.7, (L) 11.3; ζ potential: − 39.2 mV; mean diameter core (TEM): $D = 12.2$ nm.

MNP@$(CO_2Na)_1$ (MNP-1b)

MNP-1a (80 mg) in water were sonicated for 10 min, and then, Na_2CO_3 (7 mg, 0.06 mmol) was added. The suspension was sonicated during 10 min and stirred for 2 h. Then **MNP-1b** were separated by centrifugation (24 000 rpm, 20 min). The solid was washed 3 times with water, 3 more with ethanol and dried under vacuum (**MNP-1b**, 1%). Data for **MNP-1b**: TGA (%): (Fe_3O_4) 93.4, (L) 6.6; ζ potential: − 11.6 mV; mean diameter core (TEM): $D = 12.1$ nm.

MNP@$(CO_2Na)_7$ (MNP-5b)

These MNP were prepared as described above, starting from starting from **MNP-5a** (80 mg) and Na_2CO_3 (20 mg, 0.18 mmol) (**MNP-5b**, 85%). Data for **MNP-5b**: TGA (%): (Fe_3O_4) 90.1, (L) 9.9; ζ potential: − 20.5 mV; mean diameter core (TEM): $D = 12.2$ nm.

General procedure for lead capture with MNP

First, a solution of $Pb(NO_3)_2$ in water (final concentration of Pb^{2+} 0.5 g/L) and a suspension of MNP in water (1.0 g/L) were prepared. To achieve different Pb^{2+} and MNP concentrations the corresponding volume from each solution was added to an Eppendorf of 200 µL for a final volume of 150 µL. Then it was sonicated (check time for each experiment below). After that, the MNP were separated with a neodymium magnet from the supernatant that was withdrawn. Finally, the amount of lead and iron cations remaining in the supernatant was analysed by ICP.

General procedure for MNP recovery

Over the MNP obtained in the previous assays (after addition of Pb^{2+} and elimination of the supernatant) a specified volume of water and of a HNO_3 solution (3 M) was added. The final volume was 200 µL, and the final concentrations are indicated on each experiment (see below) (final pH 0.5). Then it was sonicated (check time for each experiment below). After that, the MNP were separated with a neodymium magnet from the supernatant that was withdrawn. Finally, the amount of lead and iron cations remaining in the supernatant was analysed by ICP.

MNP capture capacity of Pb^{2+} and recovery

Study of MNP capture capacity

For this purpose, several tests of lead capture were performed with a constant Pb^{2+} concentration (16.7 mg/L) and different MNP concentrations of the three synthesized MNP, unmodified **MNP-0**, modified **MNP-1b** and **MNP-5b**. To analyse the influence of the functionalization, two types of studies were carried out. In the first one, the concentration of Fe_3O_4 was kept constant for each MNP (0.10, 0.20, 0.40 and 0.80 g/L). In the second one, the amount of MNP was dependent on the equivalents of carboxylate groups, employing different molar ratios $-CO_2^-$:Pb^{2+} (1:1, 2:1, 4:1, 8:1). Thus, in these assays, the final concentrations for **MNP-0** were 0.10, 0.20, 0.40 and 0.80 g/L; for **MNP-1b** were 0.105, 0.21, 0.42, 0.84 g/L; and for **MNP-5b** were 0.11, 0.22, 0.44, 0.88 g/L.

MNP recovery study

After the process of capture, the aim is to recover MNP in order to carry out another capture process. Thus, a test of MNP recovery is carried out on the previous samples using a relationship $-CO_2^-$:Pb^{2+} of 4:1 (**MNP-0** 0.40 g/L, **MNP-1b** 0.42 g/L, **MNP-5b** 0.44 g/L and Pb^{2+} 16.7 mg/L). These relationships assure the surface saturation in the first capture

process. The effect of acid concentration (1 M and 3 M) and stirring time (5 and 15 min) was also studied. By ICP, Pb^{2+} values were obtained to determine the amount of released and the Fe values were determined to check degradation of MNP.

Cycles of lead capture and MNP recovery

For the first cycles, the conditions of the assays were different. For the first capture, it was added 20 µL of Pb^{2+} solution (0.5 Pb^{2+} g/L), 250 µL of MNP suspension (for **MNP-0** 1.0 g/l; for **MNP-5b** 1.1 g/L) and water to achieve a final volume of 1.5 mL. It was sonicated 1 min and 20 min for the magnetic separation. After that, the supernatant was isolated and analysed the amount of lead and iron cations by ICP.

Over the MNP with the lead adsorbed was added 1.5 mL of HNO_3 0.1 M. The suspension was sonicated 1 min. The supernatant was analysed by ICP once the 20 min of magnetic separation. To complete the recovery, the MNP undergo a basic treatment with 1.5 mL of Na_2CO_3 5 mM, during 1 min of sonication and 20 min of magnetic separation, to eliminate de supernatant.

To the next cycles, in the capture only was added the 20 µL of Pb^{2+} and water to achieve 1.5 mL. And for the MNP recovery and the basic treatment, the protocol was the same as that used for the first cycle.

Optimization of Pb^{2+} capture process and recovery of MNP

Once it was observed in preliminary assays that functionalization with dendritic systems had advantages with respect to MNP covered with monofunctional ligand, several functionalization experiments to anchor dendrimer on MNP were carried out taking into account magnetic separation time, capture time, stirring and acid concentration time for recovery and sonication time for dispersion (see supporting information).

Optimization of sonication time for lead capture

Capture tests are performed by keeping constant the concentration of MNP (0.40 g/L for **MNP-0** and 0.44 g/L for **MNP-5b**) and Pb^{2+} (16.7 mg/L) and varying the sonication time. Once the solution is prepared, it is placed in the ultrasonic bath for 1, 5 or 15 min; then, the supernatant is separated and analysed by ICP for the presence of lead and iron cations (Fig. S15).

Optimization of magnetic separation time

First, the time needed to achieve complete magnetic separation is optimized. Tests of capture are performed with constant concentrations of **MNP-0** (0.40 g/L) and **MNP-5b** (0.44 mg/L) and sonicated for 5 min. After this time, they are placed in the magnet rack, and samples are taken at 1, 5, 15 and 30 min. To take the samples, the supernatant is removed from the Eppendorf, and the amount of Fe remaining in suspension is analysed by ICP (Fig. S16).

Optimization of acid concentration in recovery

Capture tests are performed with a concentration for Pb^{2+} of 16.7 mg/L and 0.40 g/L for **MNP-0** and 0.44 g/L for **MNP-5b**. Afterwards, the test of MNP recovery is performed where the final concentration of the acid solution is varied using concentrations of 0.001, 0.0025, 0.01, 0.1, 1.0 and 3.0 M. The supernatants are analysed by ICP for the presence of lead and iron cations (Fig. S17).

Optimization of sonication time in the recovery of MNP

As well as for optimization of sonication time, the test of capture is carried out with constant concentrations of Pb^{2+} (16.7 mg/L) and 0.40 g/L for **MNP-0** and 0.44 g/L for **MNP-5b**. The MNP recovery test is carried out on these samples, where the sonication time is modified with ultrasound at 1, 5 and 15 min. The effect of this variable is analysed according to the ICP data performed on the supernatant (Fig. S18).

Adsorption isotherms

In this case, the concentration of the MNP suspensions was kept constants (**MNP-0** 0.40 g/L and **MNP-5b** 0.44 g/L) and lead concentrations were modified (3.3, 10.0, 16.7, 23.3, 30.0 mg/L). Each suspension was sonicated for 10 min, and then, the MNP were separated with a magnet. The supernatant was analysed by ICP to quantify the presence of lead cations (Figs. 6, 7).

Supplementary Information The online version contains supplementary material available at https://doi.org/10.1007/s13201-023-02012-2.

Acknowledgements This work was supported by the Ministry of Science and Innovation (ref. PID2020-112924RB-I00), Comunidad Autónoma de Madrid and European funding from FEDER Program (B2017/BMD-3703 (NANODENDMED II-CM)) and Grant EPU-INV/2020/014 (CAM, UAH). CIBER-BBN is an initiative funded by the VI National R&D&i Plan 2008–2011, Iniciativa Ingenio 2010, Consolider Program, CIBER Actions and financed by the Instituto de Salud Carlos III with assistance from the European Regional Development Fund.

Declarations

Conflict of interest The authors declare that they have no known competing financial interests or personal relationships that could have appeared to influence the work reported in this paper.

References

Allabashi R, Arkas M, Hormann G, Tsiourvas D (2007) Removal of some organic pollutants in water employing ceramic membranes impregnated with cross-linked silylated dendritic and cyclodextrin polymers. Water Res 41:476–486

Barrios-Gumiel A, Sepúlveda-Crespo D, Jiménez JL, Gómez R, Muñoz-Fernández MA, de la Mata FJ (2019) Dendronized magnetic nanoparticles for HIV-1 capture and rapid diagnostic. Colloids Surf B-Biointerfaces 181:360–368

Bruce IJ, Sen T (2005) Surface modification of magnetic nanoparticles with alkoxysilanes and their application in magnetic bioseparations. Langmuir 21:7029–7035

Chou C-M, Lien H-L (2011) Dendrimer-conjugated magnetic nanoparticles for removal of zinc (II) from aqueous solutions. J Nanopart Res 13:2099–2107

Galán M, Fuentes-Paniagua E, de la Mata FJ, Gómez R (2014a) Heterofunctionalized carbosilane dendritic systems: bifunctionalized dendrons as building blocks versus statistically decorated dendrimers. Organometallics 33:3977–3989

Galán M, Sánchez-Rodríguez J, Jiménez JL, Relloso M, Maly M et al (2014b) Synthesis of new anionic carbosilane dendrimers via thiol-ene chemistry and their antiviral behaviour. Org Biomol Chem 12:3222–3237

Gao Y, de Jubera AMS, Marinas BJ, Moore JS (2013) Nanofiltration membranes with modified active layer using aromatic polyamide dendrimers. Adv Func Mater 23:598–607

Hairom NHH, Soon CF, Mohamed RMSR, Morsin M, Zainal N, et al (2021) A review of nanotechnological applications to detect and control surface water pollution. Environ Technol Innov 24

Hare V, Chowdhary P, Kumar B, Sharma DC, Baghel VS (2019) Arsenic toxicity and its remediation strategies for fighting the environmental threat. In: Bharagava RN, Chowdhary P (eds) Emerging and eco-friendly approaches for waste management. Springer, Singapore, pp 143–170

Jassby D, Cath TY, Buisson H (2018) The role of nanotechnology in industrial water treatment. Nat Nanotechnol 13:670–672

Joseph L, Jun B-M, Flora JRV, Park CM, Yoon Y (2019) Removal of heavy metals from water sources in the developing world using low-cost materials: a review. Chemosphere 229:142–159

Khan FSA, Mubarak NM, Khalid M, Walvekar R, Abdullah EC et al (2020) Magnetic nanoadsorbents' potential route for heavy metals removal—a review. Environ Sci Pollut Res 27:24342–24356

Khatibikamal V, Torabian A, Panahi HA, Baghdadi M (2019) Stabilizing of poly(amidoamine) dendrimer on the surface of sand for the removal of nonylphenol from water: batch and column studies. J Hazard Mater 367:357–364

Kim KJ, Park JW (2017) Stability and reusability of amine-functionalized magnetic-cored dendrimer for heavy metal adsorption. J Mater Sci 52:843–857

Li M, Lv Z, Zheng J, Hu J, Jiang C et al (2017) Positively charged nanofiltration membrane with dendritic surface for toxic element removal. ACS Sustain Chem Eng 5:784–792

Liosis C, Papadopoulou A, Karvelas E, Karakasidis HE, Sarris IE (2021) Heavy metal adsorption using magnetic nanoparticles for water purification: a critical review. Materials 14:7500

Liu L, Huang X, Zhang X, Li K, Ji Y et al (2018) Modification of polyamide TFC nanofiltration membrane for improving separation and antifouling properties. RSC Adv 8:15102–15110

Malkoch M, García-Gallego S (2020) Dendrimer chemistry: synthetic approaches towards complex architectures. Royal Society of Chemistry

Manna P, Tiraferri A, Sangermano M, Bernstein R, Kasher R (2019) Stepwise synthesis of oligoamide coating on a porous support: fabrication of a membrane with controllable transport properties. Sep Purif Technol 213:11–18

Martinez-Boubeta C, Simeonidis K (2019) Magnetic nanoparticles for water purification. In: Thomas S, Pasquini D, Leu S, Gopakumar D (eds) Nanoscale materials in water purification. Elsevier Science BV, Berlin, pp 521–552

Masindi V, Muedi KL (2018) Environmental contamination by heavy metals. In: Hosam EMS, Refaat FA (eds) Heavy metals. InTech, pp 115–132

Moosavi S, Wei Lai C, Gan S, Zamiri S, Pivehzhan OA, Johan MR (2020) Application of efficient magnetic particles and activated carbon for dye removal from wastewater. ACS Omega 5:20684–20697

Ortega P, Sánchez-Nieves J, Cano J, Gómez R, de la Mata FJ (2020) Poly(carbosilane) dendrimers and other silicon-containing dendrimers. In: Malkoch M, Gallego SG (eds) Dendrimer chemistry: synthetic approaches towards complex architectures. Royal Society of Chemistry, pp 114–145

Parham N, Panahi HA, Feizbakhsh A, Moniri E (2018) Synthesis of high generation thermo-sensitive dendrimers for extraction of rivaroxaban from human fluid and pharmaceutic samples. J Chromatogr A 1545:12–21

Pereira RFP, Valente AJM, Burrows HD (2014) The interaction of long chain sodium carboxylates and sodium dodecylsulfate with lead(II) ions in aqueous solutions. J Colloid Interface Sci 414:66–72

Prados IM, Barrios-Gumiel A, de la Mata FJ, Marina ML, García MC (2022) Magnetic nanoparticles coated with carboxylate-terminated carbosilane dendrons as a reusable and green approach to extract/purify proteins. Anal Bioanal Chem 414:1677–1689

Qu X, Brame J, Li Q, Álvarez PJJ (2013) Nanotechnology for a safe and sustainable water supply: enabling integrated water treatment and reuse. Accounts Chemicla Res 46:834–843

Quintana-Sánchez S, Barrios-Gumiel A, Sánchez-Nieves J, Copa-Patiño JL, de la Mata FJ, Gómez R (2021) Bacteria capture with magnetic nanoparticles modified with cationic carbosilane dendritic systems. Biomater Adv. https://doi.org/10.1016/j.msec.2021.112622

Saadi R, Saadi Z, Fazaeli R, Fard NE (2015) Monolayer and multilayer adsorption isotherm models for sorption from aqueous media. Korean J Chem Eng 32:787–799

Sajid M, Nazal MK, Ihsanullah BN, Osman AM (2018) Removal of heavy metals and organic pollutants from water using dendritic polymers based adsorbents: a critical review. Sep Purif Technol 191:400–423

Shen C, Zhao Y, Li W, Yang Y, Liu R, Morgen D (2019) Global profile of heavy metals and semimetals adsorption using drinking water treatment residual. Chem Eng J 372:1019–1027

Sohail I, Bhatti IA, Ashar A, Sarim FM, Mohsin M et al (2020) Polyamidoamine (PAMAM) dendrimers synthesis, characterization and adsorptive removal of nickel ions from aqueous solution. J Materials Res Technol 9:498–506

Tanaka T, Shibata K, Hosokawa M, Hatakeyama K, Arakaki A et al (2012) Characterization of magnetic nanoparticles modified with thiol functionalized PAMAM dendron for DNA recovery. J Colloid Interface Sci 377:469–475

Tremblay-Parrado K-K, García-Astrain C, Avérous L (2021) Click chemistry for the synthesis of biobased polymers and networks derived from vegetable oils. Green Chem 23:4296–4327

Vasquez-Villanueva R, Peña-González CE, Sánchez-Nieves J, de la Mata FJ, Marina ML, García MC (2019) Gold nanoparticles coated with carbosilane dendrons in protein sample preparation. Microchim Acta 186:508

Wadhawan S, Jain A, Nayyar J, Mehta SK (2020) Role of nanomaterials as adsorbents in heavy metal ion removal from waste water: a review. J Water Process Eng 33:101038

Wang D, Hubacek K, Shan YL, Gerbens-Leenes W, Liu JG (2021) A review of water stress and water footprint accounting. Water 13:201

Xi W, Scott TF, Kloxin CJ, Bowman CN (2014) Click chemistry in materials science. Adv Funct Mater 24:2572–2590

Yen CH, Lien HL, Chung JS, Yeh HD (2017) Adsorption of precious metals in water by dendrimer modified magnetic nanoparticles. J Hazard Mater 322:215–222

Yuan BB, Zhao SC, Hu P, Cui JB, Niu QJ (2020) Asymmetric polyamide nanofilms with highly ordered nanovoids for water purification. Nat Commun 11:6102

Zarei A, Saedi S, Seidi F (2018) Synthesis and application of Fe_3O_4@SiO_2@carboxyl-terminated PAMAM dendrimer nanocomposite for heavy metal removal. J Inorg Organomet Polym Mater 28:2835–2843

Zhang X, Qian J, Pan B (2016) Fabrication of novel magnetic nanoparticles of multifunctionality for water decontamination. Environ Sci Technol 50:881–889

Zheng H, Cooper DR, Porebski PJ, Shabalin IG, Handing KB, Minor W (2017) CheckMyMetal: a macromolecular metal-binding validation tool. Acta Crystallographica Sect D Struct Biol 73:223–233

Zia M, Phull AR, Ali JS (2016) Challenges of iron oxide nanoparticles. Powder Technol 7:49–67